

MR Detection of Mechanical Vibrations Using a Radiofrequency Field Gradient

Nathalie Baril,* Czeslaw Jozef Lewa,† Jacques Donald de Certaines,‡ Paul Canioni,*
Jean-Michel Franconi,* and Eric Thiaudière*,¹

*Magnetic Resonance Centre, CNRS-Université Victor Segalen Bordeaux 2, Bordeaux, France; †Department of Physics, University of Gdansk, Gdansk, Poland; and ‡Magnetic Resonance in Biology and Medicine, IFR 91, Université Rennes I, Rennes, France

Received April 11, 2001; revised September 24, 2001; published online November 29, 2001

A new method for NMR characterization of mechanical waves, based upon radiofrequency field gradient for motion encoding, is proposed. A binomial B_1 gradient excitation scheme was used to visualize the mobile spins undergoing a periodic transverse mechanical excitation. A simple model was designed to simulate the NMR signal as a function of the wave frequency excitation and the periodicity of the NMR pulse sequence. The preliminary results were obtained on a gel phantom at low vibration frequencies (0–200 Hz) by using a ladder-shaped coil generating a nearly constant RF field gradient along a specific known direction. For very small displacements and/or B_1 gradients, the NMR signal measured on a gel phantom was proportional to the vibration amplitude and the pulse sequence was shown to be selective with respect to the vibration frequency. A good estimation of the direction of vibrations was obtained by varying the angle between the motion direction and the B_1 gradient. The method and its use in parallel to more conventional MR elastography techniques are discussed. The presented approach might be of interest for noninvasive investigation of elastic properties of soft tissues and other materials. © 2002 Elsevier Science

Key Words: radiofrequency field gradient; vibrations.

INTRODUCTION

Radiofrequency field gradients were proposed as an alternative to static magnetic field gradients for spatial encoding in MRI. Such gradients are presently used for MR microscopy ($I-3$) or diffusion measurements ($3-5$). Recently it was shown that two-dimensional B_1 imaging was possible on planar objects without any use of the static field gradient (6). The advantages of B_1 over B_0 imaging lie in a reduction of eddy current artifacts, due to the B_0 gradient switching, in a lower sensitivity to magnetic susceptibility artifacts and a simplification of the instrumentation required.

NMR can be used to measure the elastic properties of matter. The knowledge of the wavelength, the celerity, and the amplitude of a propagating mechanical wave can lead to the derivation

of Young's modulus and the dispersion pattern. NMR characterization of viscoelastic properties of matter may constitute a beneficial alternative to other methods (7) because of its noninvasiveness and its potential application to clinical purposes (new diagnostic techniques and tissue characterization for computed surgery). MR elastography could also be applied to other materials (biomaterials, composites, . . .), when the assessment of their mechanical properties is of critical importance. Another advantage of NMR detection of mechanical waves is the possibility of receiving signals from relatively deep parts of the object or the subject under investigation.

Several theoretical approaches have dealt with the use of static field gradients for the determination of viscoelastic properties by MRI. The principles of those methods consisted of imaging displacements induced by a mechanical wave using a Larmor frequency modulation ($8, 9$) or by changing the phase of the transverse magnetization ($10, 11$). Successful applications of the theoretical developments were achieved on gel phantoms, where the elasticity modulus and the refraction pattern of transverse mechanical waves were imaged ($12, 13$). MRI of transverse strain waves was also carried out on human calf muscle (14). Another motion-sensitive MR method based upon sinusoidal modulation of B_0 gradients allowed imaging at ultrasonic frequencies ($15, 16$). A further development in B_0 fast imaging of propagating waves was achieved without synchronizing the oscillating gradients with the mechanical stimulation (17).

The latter work opened the way for spectroscopic investigations of such waves, i.e., their resonance character and directional selectivity. From another theoretical study, it was shown that spectroscopic elastography (18) could also be assessed by tuning the gradient oscillation frequency with respect to the vibration frequency.

Spin motions, such as diffusion, perfusion, and slow fluid flow, can be detected using radiofrequency field gradients ($19, 20$). However, to our knowledge there is no report on the use of B_1 gradients applied to spectroscopic MR elastography. The advantages of B_1 over B_0 techniques are the following: (i) the absence of acoustic noise induced by gradient coil switching; (ii) a reduction of eddy currents induced by fast switching rates; and (iii) a

¹ To whom correspondence should be addressed. E-mail: thiaudiere@rmsb.u-bordeaux2.fr.

decrease in hardware requirements. The goal of the present study is to introduce an alternative NMR detection method in order to characterize mechanical waves by using a B_1 radiofrequency field gradient instead of a B_0 gradient. The basis of this new method is the application of RF gradient pulses with alternating phases. As a consequence, mobile spins experience a variable excitation scheme resulting in a modulation of the MR signal magnitude as a function of the frequency, the amplitude, and the direction of the displacement. Results obtained on a gel phantom were in agreement with the theoretical background and validate this new approach to MR elastography.

METHODS

Experimental Setup

A wave generator (Yokogawa, Tokyo, Japan) produced a sine function amplified by a common audio stereophonic 100-W amplifier. The root mean square (RMS) voltage after amplification was measured by an oscilloscope (Tektronics, Inc., Beaverton, OR). The amplified sine wave was converted into vibration by a homemade exciter. The vibrations were transmitted via a rigid fiberglass rod to a plate incorporated into a gel phantom (10) included into a polystyrene box. The phantom was then positioned at the isocenter of the magnet for NMR experiments (Fig. 1).

To convert the amplified voltage into a vibration amplitude, a calibration of the exciter was carried out using a laser beam produced by a 0.5-mW helium–neon laser operating at 632.8 nm (Melles Griot, Carlsbad, CA). The beam was reflected by a mir-

ror installed on the vibrating exciter and measured by a CCD (charge-couple device) detector (1024 pixels, Ulice Optronique, Gif-sur-Yvette, France). The vibration amplitude was then calculated from the CCD detector signal. By systematically varying both the voltage and the frequency of the input wave a very accurate calibration of the exciter was ensured.

NMR Experiments

Experiments were performed using a Bruker Biospec 47/50 (Bruker Medical, Karlsruhe, Germany) equipped with a 50-cm-bore superconducting magnet operating at 4.7 T. A homemade ladder-shaped coil tuned at the proton resonance frequency, 200.3 MHz, was positioned 2 cm from the gel phantom. The coil operated in the transmit/receive mode with its main axis parallel to B_0 . Detailed information on this ladder-shaped coil is given in Ref. (6). The NMR acquisition was triggered by an external 5-V TTL (transistor transistor logical) signal in phase with the sine function used for the exciter. Water proton free induction decays (1024 data points, 500-Hz sweep width, 5-s recovery delay) were Fourier transformed. Spectra were then analyzed separately using Igor Pro (Wavemetrics, Lake Oswego, OR) data processing software. This software was also used for the calculations described in the next section.

THEORY

One-dimension space encoding may be achieved by the quasi-constant radiofrequency field gradient produced by the ladder-shaped coil (6). The application of a first rectangular RF pulse with a phase φ can be thought of as a nonhomogenous excitation of the sample in which the transverse magnetization can be described as

$$M_{x',y'} = M_0(z) \cdot \sin(\gamma G_{1\varphi} T_p \cdot z), \quad [1]$$

where $x'y'$ are the rotating frame coordinates, $M_0(z)$ the equilibrium magnetization at position z , γ the magnetogyric ratio of the spin, $G_{1\varphi}$ the RF gradient along the z direction, and T_p the RF pulse length. Neglecting off-resonance effects and relaxation processes, the application of a second RF pulse with the same duration but an opposite phase ($-\varphi$) is expected to achieve the recovery of the longitudinal magnetization, as long as the spins are stationary. Thus a null magnetization at the carrier frequency should be observed after such a simple binomial excitation.

Then let us assume that a sinusoidal mechanical vibration induces an oscillatory motion within the sample. The position of each spin after a time t can be described as

$$z(t) = z_0 + A \cdot \sin(\omega \cdot t + \phi), \quad [2]$$

where z_0 is the position of the spin without vibration, A is the

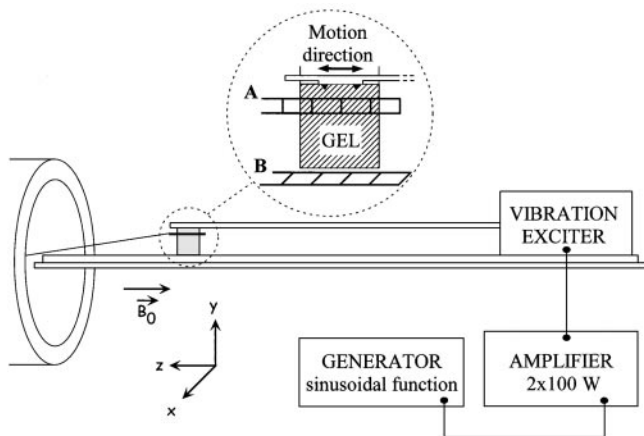


FIG. 1. Experimental setup. A sinusoidal signal was generated, amplified, and transmitted to the vibrating exciter. It was connected by a rigid rod to a $5 \times 2\text{-cm}^2$ plate which was incorporated in the gel. Upon excitation along the z axis, transverse waves were generated and detected using the ladder-shaped coil with its main axis parallel to the motion of the plate. The NMR coil was positioned in (A) for the experiments of Figs. 4 and 5 and in (B) for the experiments of Fig. 6. The distance between the gel box and the coil was 2 cm and no contact between them was allowed.

vibration amplitude, ω is the motion pulsation, and ϕ is the constant phase shift.

The effect of motion on the magnetization flip angle distribution within the sample during a rectangular RF pulse can be written as

$$\alpha_n = \alpha_{n-1} + \int_{t_{n-1}}^{t_n} \gamma \cdot G_1 \cdot (z_0 + A \cdot \sin(\omega \cdot t + \phi)) \cdot dt, \quad [3]$$

where α_n is the flip angle of the spin at position z_n and at time t_n , and α_{n-1} is the flip angle of the spin at position z_{n-1} and at time t_{n-1} . The pulse length is then $(t_n - t_{n-1})$.

Integration of Eq. [3] over t gives

$$\alpha_n = \alpha_{n-1} + \gamma \cdot G_1 \cdot z_0 T_p + \gamma \cdot G_1 \cdot \frac{A}{\omega} [\cos(\omega \cdot t_{n-1} + \phi) - \cos(\omega \cdot t_n + \phi)]. \quad [4]$$

Equation [4] can be used to predict the flip angle distribution of a vibrating sample immediately after the spin excitation produced by a rectangular RF pulse. In the case of a sequence of RF pulses, the evolution of the positions of the spins during the delays separating the pulses can be calculated using Eq. [2]. Thus the flip angle distribution at the end of the pulse sequence can be modeled in an iterative manner by alternating calculations with Eqs. [2] and [4]. The total normalized signal S corresponding to a given flip angle distribution is then

$$S = \frac{1}{z_m} \int_0^{z_m} M_0(z) \sin \alpha(z) dz \quad [5]$$

for spins present within a distance z_m .

One simple pulse sequence can be designed in order to detect the vibration frequency of the spins: $(\tau - \alpha_{(\varphi)} - \tau - \alpha_{(-\varphi)})_n$, where τ is the interpulse delay, φ the pulse phase, and n the number of loops. For a single spin system (e.g., water protons excited on-resonance), if the period of the loop is equal to the period of the vibration and if the vibration phase ϕ is equal to zero, one expects a constant flip angle within the whole sample which is amplified each time the number of the loop is incremented. The total signal is then $M_0 \cdot \sin(\alpha)$, a value that can be approximated to $M_0 \cdot \alpha$ for very small flip angles, i.e., for very low vibration amplitudes. In such a case, the NMR signal may be taken as proportional to the vibration amplitude. For accurate measurements, there must be no signal (neglecting diffusion processes) at the carrier frequency in the absence of vibration. Using the experimental setup described above (see Methods) it was not possible to reach an acceptable cancellation of the NMR signal for a loop number of 16. This could be due to an imperfect RF pulse; therefore the basic sequence was changed to that depicted in Fig. 2, where a binomial $1\bar{3}3\bar{1}$ pulse was chosen. The total recovery time was

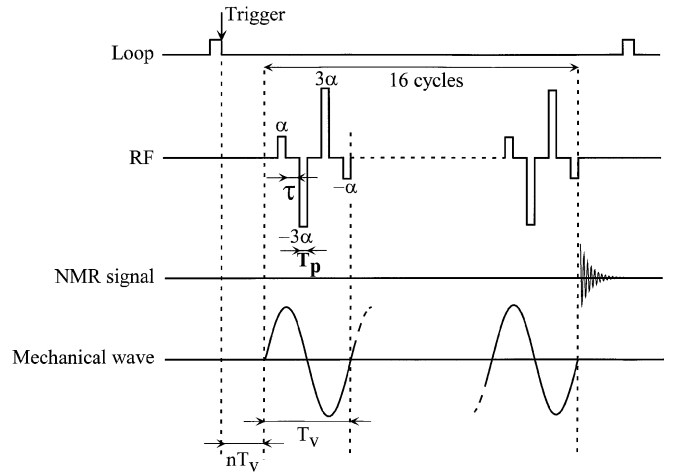


FIG. 2. Gradient pulse sequence. Four B_1 gradient pulses of length T_p were generated and interspersed with delays τ . The binomial shape $1\bar{3}3\bar{1}$ was cycled 16 times with a characteristic period $T_v = 4(T_p + \tau)$ matched to the vibration period. For appropriate detection, a trigger signal was generated in-phase with the wavefunction. Also shown is the vibration wave in-phase with the pulse sequence.

set to an integer multiple of the vibration period in order to avoid unwanted dephasing.

Figure 3 shows the calculation from Eqs. [2] and [4] of the expected NMR response for a spin system oscillating at an operating frequency of 0–280 Hz. The pulse sequence was cycled at a period of $(1/60)$ s with a gradient pulse of 1 ms and interpulse delays of 3.1667 ms. The number of loops was 16. Clearly a well-resolved line was visible at a vibration frequency of 60 Hz, corresponding to the characteristic pulse sequence

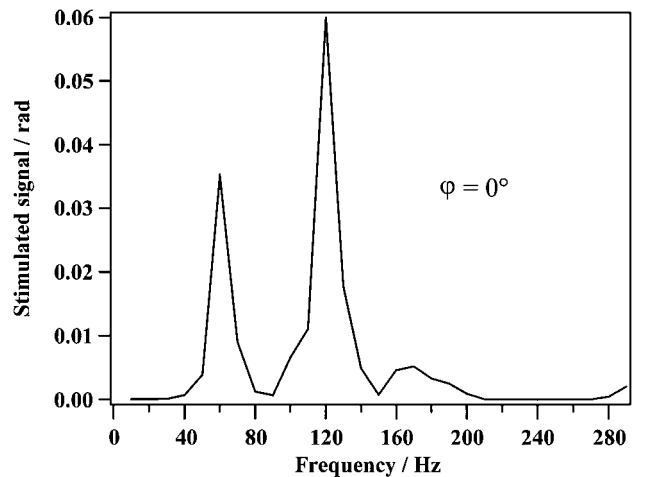


FIG. 3. Theoretical simulation of the NMR detection of a mechanical wave using the sequence depicted in Fig. 2. Input parameters: $G_1 = 40 \mu\text{T/m}$ for the α pulse, A (vibration amplitude) = $504 \mu\text{m}$, $T_p = 1 \text{ ms}$, $\tau = 3.1667 \text{ ms}$, corresponding to a characteristic pulse sequence period of 60 Hz. The result is represented according to Eq. [5] with the equilibrium magnetization M_0 set to unity.

cycling time. It was noticed that vibration frequencies of 120 and 180 Hz could also be detected with this sequence. However, only the lowest detectable frequency for a given pulse sequence period will be taken into account under Results and Discussion. Several simulations were carried out for different loop periods and various loop numbers. It was clear that increasing the number of repetitions (n) of the basic pulse sequence resulted in a better frequency selectivity of the vibration modes. This behavior was in good agreement with the excitation bandwidth estimated by Fourier transformation of the pulse sequence chronogram for various pulse lengths, interpulse delays, and numbers of loops (not shown).

RESULTS

In order to confirm the principles of NMR detection of transverse vibrations using a radiofrequency field gradient, several experiments were carried out using the experimental setup described in Fig. 1. The characteristic period of the pulse sequence was matched to a vibration frequency of 60 Hz, as described under Theory. As a control measurement, the NMR signal cancellation was checked at the null vibration frequency. The vibration frequency was then incremented from 40 to 200 Hz. The result of such an experiment is reported in Fig. 4. It must be mentioned that the NMR data were corrected for the intrinsic response of the vibrating exciter (see Methods). From Fig. 4, it is clear that the 60-Hz vibration mode was well detected together with a correct frequency selection. The 120-Hz mode (2ν) was also well detected but to a lesser extent as compared to what was expected from the theoretical simulation presented in Fig. 3. Moreover the 180-Hz mode (3ν) was barely detected.

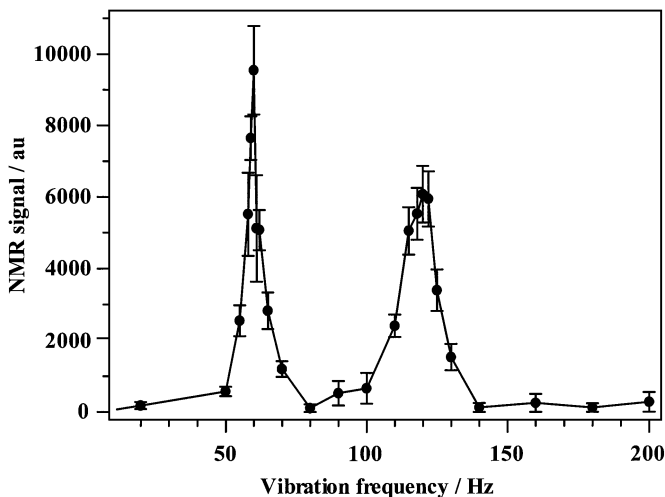


FIG. 4. Experimental NMR detection of transverse waves for various vibration frequencies. The experimental setup is described in Fig. 1. The vibration amplitude of the plate incorporated in the gel was 0.16 mm. NMR signals derived from magnitude spectra were obtained with the pulse sequence depicted in Fig. 2. Pulse length T_p was 1 ms and τ was 3.1667 ms. G_1 was $13 \mu\text{T/m}$ for the α pulse.

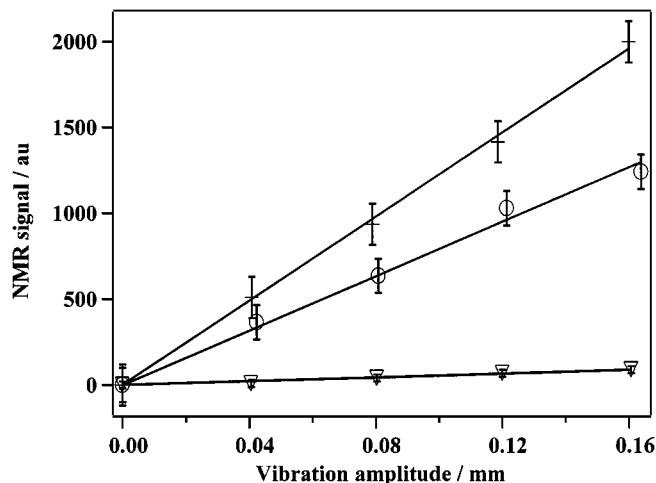


FIG. 5. NMR response as a function of the vibration amplitude. The vibration frequencies were 60 Hz (crosses), 120 Hz (circles), and 180 Hz (triangles). In each case, the pulse sequence characteristic period was matched to the vibration period with $T_p = 1$ ms and $\tau = 3.1667$ ms (60 Hz), $\tau = 1.083$ ms (120 Hz), and $\tau = 0.389$ ms (180 Hz). Solid lines represent the fit to a straight-line function.

Obviously, the gel itself could be at the origin of dispersion processes that might decrease the vibration amplitude at higher frequencies. Other experiments with a pulse sequence period in the range of 40–80 Hz also showed the same kind of response at ν and 2ν (not shown).

In order to assess that the NMR signal was quantitatively correlated to the vibration amplitude, experiments at constant frequencies and variable exciter amplitudes were carried out. This was possible because of a careful calibration of the vibrating exciter (see Methods). For each vibration frequency (60, 120, and 180 Hz) the characteristic period of the pulse sequence was matched accordingly with the constant RF pulse length (1 ms) and adequate interpulse delays. Figure 5 shows that the NMR response increased almost linearly as a function of the vibration amplitude. This linearity indicated that the product $\gamma \cdot G_1 \cdot T_p \cdot z$ was small enough to allow the approximation $\sin \alpha = \alpha$. This was confirmed with other experiments where the G_1 gradient and/or the exciter amplitudes were higher: then the linearity was no longer observed. Again, the slopes of the fitting lines of Fig. 5 are frequency dependent, indicating that the actual motion amplitude in the gel was different from that of the exciter.

The ladder-shaped RF coil used in this study was designed to produce a quasi-constant B_1 -gradient along its main axis, with other gradients remaining in a perpendicular direction that we will call y (details are given in Ref. (6)). These additional gradients were shown (from both a theoretical and experimental point of view) to be symmetrical with respect to the main axis of the coil. Thus if the coil is centered at a position $y = 0$ for convenience, it can be shown that $G_1(y) = -G_1(-y)$. For a direction of mechanical vibration parallel to y , the NMR signal arising from the ($+y$) region should be cancelled by the NMR signal arising from the ($-y$) region. In other words, an oscillatory

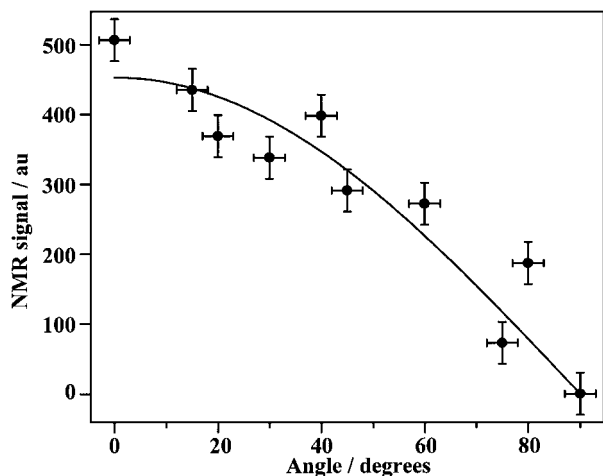


FIG. 6. Directional dependence of the NMR detection. The ladder-shaped coil was moved in the (xz) plane about the y axis. The angles reported in the graph refer to the direction of motion that was parallel to the z axis. The vibration frequency was 60 Hz and the vibration amplitude was 0.36 mm. The solid line is the fit to a cosine function.

motion along the main axis of the coil should be detected whereas no signal should be recorded from vibrations perpendicular to the main coil axis. Despite the difficulties in gathering the results (mainly because the experimental setup was quite cumbersome with respect to the magnet diameter), the confirmation of this idea is given in Fig. 6, where the orientation of the coil was varied from 0° to 90° with respect to the motion direction. Even though the experimental data were quite spread out, the angular dependence could reasonably be fit to a cosine function. Thus, there is both frequency and directional selectivity for the detection of mechanical waves using RF gradients.

DISCUSSION

The present work deals with an alternative method for characterizing transverse mechanical waves in a homogenous medium by using radiofrequency field gradients. This is the first report on the use of RF pulses for assessing the frequency, the amplitude, and the direction of an oscillatory motion. The main goal of this study was to validate in the simplest way the physical principles of this method, i.e., by measuring the NMR response in a homogenous gel. One has to notice that the vibration parameters were obtained from spectroscopic data. Further developments are required to extend the method to MR imaging and are beyond the scope of this report. The most direct way to show the feasibility of such an approach was to synchronize the mechanical vibration with the RF pulse sequence (Fig. 2). The latter was designed with binomial compensated pulses interspersed with delays in such a way that the period of the pulse sequence coincided with the vibration frequency. When this sequence was repeated enough, a good frequency selectivity was obtained (Figs. 3 and 4). A drawback of this method was that a

trigger signal, in-phase with the mechanical wave, was necessary to obtain measurable NMR signals. However, by systematically varying the phase shift between the vibration and the NMR pulse sequence, it was easy to capture the highest NMR signal in a very reproducible way (data not shown). Thus, the identification of an unknown frequency mode within a sample is feasible by varying the pulse period and the trigger phase shift. At present, only very low frequencies (0–200 Hz) were attainable. Such a limitation was due to the radiofrequency amplification used in this study, which did not enable the use of very short and intense RF pulses in order to decrease the pulse cycling time. A more powerful RF transmitter is required to increase the frequency domain in experiments carried out on our spectrometer operating at 4.7 T. Since the measurements can be made without the need of the B_0 gradient unit, the technique may be used with simplicity on cheaper NMR systems. Besides, the method can easily be implemented on standard NMR systems operating at a lower static field (1.5 T or lower): in such cases, a lower RF power is required and the RF hardware specifications enable a much higher RF gradient switching rate (>10 kHz). Moreover a higher bandwidth would be of interest for investigating the frequency response of the material. Indeed, the gel used here did not exhibit a constant vibration amplitude as a function of the input frequency. The understanding of this behavior is important for the characterization of the viscoelastic properties of the material. The systematic study of the frequency dependence of the vibration amplitude for standard materials is planned as well as a comparison with other physical methods.

An important contribution of this work was the estimation of the direction of vibration. As seen from Fig. 6, the ladder-shaped coil made it possible to cancel the NMR detection when its main axis was normal to the direction of motion. On the other hand, it seemed difficult to determine the direction of propagation, another important parameter of a vibrating medium. In the past few years the use of B_0 imaging on clinical MRI systems made it possible to detect the direction of propagation, but not the direction of vibration. A more complete description of the viscoelastic properties of matter would be achieved in combining both B_0 and B_1 capabilities. RF-encoded motions during an external mechanical stimulation could then be imaged in a classical way by B_0 imaging. The major advantage of such a procedure is the elimination of artifacts from the sound produced by the gradient coils. This opens the way for the use of acoustic waves as an external mechanical stimulation. Even though numerous technical difficulties remain to be solved, this approach would be of interest in various clinical applications.

ACKNOWLEDGMENTS

We are grateful to Gérard Raffard and Richard Rouland for technical assistance and Pr. Laurent Sarger (CPMOH, Université de Bordeaux 1) who provided the optical equipment. This work was supported by the Conseil Régional d'Aquitaine. C. J. Lewa was supported by the University of Gdansk Grant BW 5200-5-0211-1.

REFERENCES

1. P. Maffei, P. Mutzenhardt, A. Retournard, B. Diter, R. Raulet, J. Brondeau, and D. Canet, NMR microscopy by radiofrequency field gradients, *J. Magn. Reson. A* **107**, 40–49 (1994).
2. R. Raulet, D. Grandclaude, F. Humbert, and D. Canet, Fast NMR imaging with B_1 gradients, *J. Magn. Reson.* **124**, 259–262 (1997).
3. D. Canet, Radiofrequency field gradient experiments, *Progr. NMR Spectrosc.* **30**, 101–135 (1997).
4. D. Canet, B. Diter, A. Belmajdoub, J. Brondeau, J. C. Boubel, and K. Elbayed, Self-diffusion measurements using a radiofrequency field gradient, *J. Magn. Reson.* **81**, 1–12 (1989).
5. F. Humbert, M. Valtier, A. Retournard, and D. Canet, Diffusion measurements using rf field gradient: Artifacts, remedies, practical hints, *J. Magn. Reson.* **134**, 245–254 (1998).
6. N. Baril, E. Thiaudière, B. Quesson, C. Delalande, P. Canioni, and J. M. Franconi, Single-coil surface imaging using a radiofrequency field gradient, *J. Magn. Reson.* **146**, 223–227 (2000).
7. Y. C. Fung, “Biomechanics: Mechanical Properties of Living Tissues,” Springer-Verlag, Berlin (1981).
8. C. J. Lewa, Magnetic resonance Imaging in presence of mechanical waves, *Spectrosc. Lett.* **24**, 55–67 (1991).
9. C. J. Lewa, MRI response in the presence of mechanical waves, *Acustica* **77**, 43–45 (1992).
10. C. J. Lewa and J. D. de Certaines, Visco-elastic property detection by elastic displacement NMR measurements, *J. Magn. Reson. Imaging* **6**, 652–656 (1996).
11. C. J. Lewa and J. D. de Certaines, Imaging of visco-elastic properties, *J. Magn. Reson. Imaging* **5**, 242–244 (1995).
12. R. Muthupillai, D. J. Lomas, P. J. Rossman, *et al.*, Magnetic resonance elastography by direct visualization of propagating acoustic strain waves, *Science* **269**, 1854–1857 (1995).
13. R. Muthupillai and R. L. Ehman, Magnetic resonance elastography, *Nature Med.* **2**, 601–603 (1996).
14. R. Muthupillai, P. J. Rossman, D. J. Lomas, J. F. Greenleaf, S. J. Riederer, and R. L. Ehman, Magnetic resonance imaging of transverse acoustic strain waves, *Magn. Reson. Med.* **36**, 266–274 (1996).
15. C. L. Walker, F. S. Foster, and D. B. Plewes, Magnetic resonance imaging of ultrasonic fields, *Ultrasound Med. Biol.* **24**, 137–142 (1998).
16. D. B. Plewes, S. Silver, B. Starkoski, and C. L. Walker, Magnetic resonance imaging of ultrasonic fields; gradient characteristics, *J. Magn. Reson. Imaging* **11**, 452–457 (2000).
17. C. J. Lewa, M. Roth, M. Nicol, J. M. Franconi, and J. D. de Certaines, A new fast and unsynchronised method for MRI of visco-elastic properties of soft tissues, *J. Magn. Reson. Imaging* **12**, 784–789 (2000).
18. C. J. Lewa, Elasto-magnetic resonance spectroscopy, *Europhys. Lett.* **35**, 73 (1996).
19. G. S. Karczmar, D. B. Twieg, T. J. Lawry, G. B. Matson, and M. W. Weiner, Detection of motion using B_1 gradient, *Magn. Reson. Med.* **7**, 111–116 (1988).
20. G. S. Karczmar, N. J. Tavares, and M. E. Moseley, Use of radiofrequency field gradients to image blood flow and perfusion in vivo, *Radiology* **172**, 363–366 (1989).